



THE UNIVERSITY *of* EDINBURGH

## Edinburgh Research Explorer

# FM-Sim: A Hybrid Protocol Simulator of Fluorescence Microscopy Neuroscience Assays with Integrated Bayesian Inference

### Citation for published version:

Stewart, D, Cousin, M & Gilmore, S 2014, FM-Sim: A Hybrid Protocol Simulator of Fluorescence Microscopy Neuroscience Assays with Integrated Bayesian Inference. in *Computational Methods in Systems Biology: 12th International Conference, CMSB 2014, Manchester, UK, November 17-19, 2014, Proceedings*. Lecture Notes in Computer Science, vol. 8859, Springer International Publishing, pp. 248-251, Third International Workshop on Hybrid Systems Biology , Vienna, Austria, 23/07/14. [https://doi.org/10.1007/978-3-319-27656-4\\_10](https://doi.org/10.1007/978-3-319-27656-4_10)

### Digital Object Identifier (DOI):

[10.1007/978-3-319-27656-4\\_10](https://doi.org/10.1007/978-3-319-27656-4_10)

### Link:

[Link to publication record in Edinburgh Research Explorer](#)

### Document Version:

Peer reviewed version

### Published In:

Computational Methods in Systems Biology

### General rights

Copyright for the publications made accessible via the Edinburgh Research Explorer is retained by the author(s) and / or other copyright owners and it is a condition of accessing these publications that users recognise and abide by the legal requirements associated with these rights.

### Take down policy

The University of Edinburgh has made every reasonable effort to ensure that Edinburgh Research Explorer content complies with UK legislation. If you believe that the public display of this file breaches copyright please contact [openaccess@ed.ac.uk](mailto:openaccess@ed.ac.uk) providing details, and we will remove access to the work immediately and investigate your claim.



# FM-Sim : A Hybrid Protocol Simulator of Fluorescence Microscopy Neuroscience Assays with Integrated Bayesian Inference

Donal Stewart<sup>1</sup>, Stephen Gilmore<sup>2</sup>, and Michael A. Cousin<sup>3</sup>

<sup>1</sup> Doctoral Training Centre in Neuroinformatics and Computational Neuroscience,  
School of Informatics, University of Edinburgh, Edinburgh, Scotland  
donal.stewart@ed.ac.uk

<sup>2</sup> Laboratory for Foundations of Computer Science,  
School of Informatics, University of Edinburgh, Edinburgh, Scotland  
stephen.gilmore@ed.ac.uk

<sup>3</sup> Centre for Integrative Physiology,  
School of Biomedical Sciences, University of Edinburgh, Edinburgh, Scotland  
M.Cousin@ed.ac.uk

**Abstract.** We present FM-Sim, a domain-specific simulator for defining and simulating fluorescence microscopy assays. Experimental protocols as performed *in vitro* may be defined in the simulator. The defined protocols then interact with a computational model of presynaptic behaviour in rodent central nervous system neurons, allowing simulation of fluorescent responses to varying stimuli. Rate parameters of the model may be obtained using Bayesian inference functions integrated into the simulator, given experimental fluorescence observations of the protocol performed *in vitro* as training data. These trained protocols allow for predictive *in silico* modelling of potential experimental outcomes prior to time-consuming and expensive *in vitro* studies.

## 1 Introduction

Synaptic vesicle recycling at the pre-synaptic terminal of neurons is essential for the maintenance of neurotransmission at central synapses. Among the tools used to visualise the mechanics of this process is time-series fluorescence microscopy. Fluorescent dyes such as FM1-43, or engineered fluorescent versions of synaptic vesicle proteins such as pHluorins, have been employed to reveal different steps of this key process. These tools have been applied to a number of animal models, notably the neurons within the central nervous system in rodents.

Predictive *in silico* modelling of potential experimental outcomes is a highly informative procedural step prior to making the significant investment of time and expense which is needed to prepare and run an *in vitro* study. FM-Sim is a hybrid stochastic simulator written specifically for this domain. It allows the definition of many of the experimental assays which are commonly used in this field, and simulates them against a computational model of the current understanding of the mechanisms of synaptic vesicle recycling.

If experimental observation data is available from *in vitro* fluorescence microscopy assays, then simulated time-series output from the computational model may be checked for its distance from the observations, and rate parameters can be automatically inferred to fit the provided observations. FM-Sim will provide high predictive power in studies examining presynaptic function.

The main benefit of simulations performed by FM-Sim over those performed by generic stochastic simulators is that FM-Sim manages the effects of nested and overlapping events which impact on the kinetics of vesicle recycling. For example, a chemical inhibitor may be introduced at some time during an experimental protocol, with electrical stimulation applied subsequently for part of the time that the inhibitor is available. Additionally, FM-Sim can simulate a number of *in vitro* techniques used to modify the fluorescence output during an experiment.

## 2 Biological background

The domain of interest to this study is the presynaptic terminal of central nervous system neurons, as found in experimental animal models such as rodents. This is an active domain of experimental study, where the research goal is to discover the mechanisms which control the processing of synaptic vesicles within chemical synapses.

### 2.1 The Synaptic Vesicle Cycle

Within chemical synapses of central nervous system (CNS) neurons, neurotransmitter is released from the presynaptic terminal to propagate the neural signal to the postsynaptic terminal of the following neuron. This neurotransmitter is stored in vesicles within the presynaptic terminal, which are exocytosed in response to an incoming action potential. These vesicles are classed as being within pools denoting their availability for release via exocytosis: the *readily releasable pool* consists of vesicles ready to be released immediately, while the *reserve pool* consists of vesicles filled with neurotransmitter, but not close enough to the plasma membrane for immediate release.

To prevent depletion of these vesicle pools, compensatory endocytosis of plasma membrane allows regeneration of these vesicles. Two forms are studied within CNS nerve terminals:

- **Clathrin Mediated Endocytosis (CME)** [16] is the primary mechanism of membrane recovery during periods of normal levels of nerve stimulation. Individual vesicles are reconstructed directly from the plasma membrane. Following reacidification of the vesicle contents and refilling with neurotransmitter, these vesicles rejoin the reserve and readily releasable pools.
- **Activity Dependent Bulk Endocytosis (ADBE)** [9] is a second endocytosis mechanism triggered by periods of high stimulation. Here, large areas of plasma membrane are endocytosed as endosomes, which are later broken down into individual vesicles for reuse.

The mechanisms of both of these forms of endocytosis are currently subjects of detailed study.

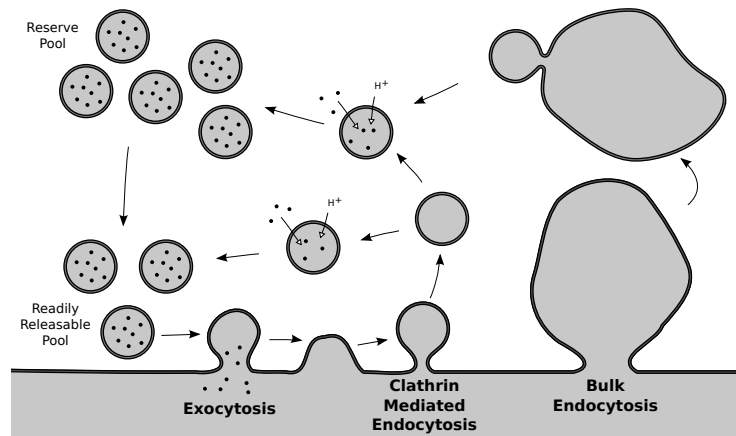


Fig. 1: The synaptic vesicle cycle.

## 2.2 Fluorescence Microscopy Imaging

Time-series fluorescence microscopy is one of the experimental procedures used to study the mechanisms of the synaptic vesicle cycle. Fluorescent probes added to nerve terminals allow us to obtain time-series images of nerve terminal behaviour under stimulation. The two commonly-used forms of fluorescent probes are FM dyes, and engineered fluorescent synaptic vesicle proteins such as pHluorins.

- **FM dyes** [8] are soluble dyes added to the extracellular media. They fluoresce when bound to membrane. If a nerve terminal is stimulated when the dye is present in the extracellular media around the neuron, the dye is taken up within vesicles and endosomes during endocytosis. Subsequent washing of the neuron removes all extracellular dye, leaving only the dye within the nerve terminal structures to fluoresce. During exocytosis, this dye is released back into the extracellular media and removed from view, which allows tracking of exocytosis rates. Different FM dyes have different uptake rates depending on the type of endocytosis. This allows isolation of the behaviour of the different forms of endocytosis. Two commonly-used dyes are FM1-43 and FM2-10.
- **pHluorins** [17, 18] are synaptic vesicle proteins fused to a fluorescent protein. These fluoresce only at neutral pH  $\approx 7.4$  (as found in the extracellular media), and do not fluoresce at low pH levels  $\approx 5.5$  (as found in reacidified vesicles). Over time the vesicles are endocytosed and reacidified causing a change in the level of fluorescence which can be used to track activity in the synaptic vesicle cycle.

Images taken during an experimental assay show many terminals of a neuron simultaneously. At the imaging resolutions which are commonly used, an individual synaptic terminal appears as a single bright area a few pixels in diameter and thus only the fluorescence of the terminal as a whole can be measured. Ingenuity in experimental design is required to deconstruct this single measure per nerve terminal to highlight the mechanisms of the synaptic vesicle cycle.

Different aspects of the synaptic vesicle cycle can be isolated and studied by using either FM dyes or pHluorins in combination with chemical inhibitors, or on various genetic knockdown animal models.

For example, adding the reacidification inhibitor Bafilomycin A1 to a pHluorin assay prevents the quenching of the fluorescent marker following endocytosis [3], offering further opportunities to isolate parts of the synaptic vesicle recycling process.

### 3 Computational Modelling Opportunity

This domain has already been the subject of computational modelling research. Prior work has included a study by [3] fitting ODEs to experimental results of vesicle reacidification. This has yielded a detailed kinetic model for the reacidification step of vesicle recycling. A paper by [11] used experimental data showing vesicle release depression over extended stimulation to iteratively construct an ODE model representing the rate limiting steps in vesicle trafficking. A study by [14] fitted a system of ODEs representing a model of vesicle recycling to experimental data observed in cultured hippocampal neurons. The model illustrated the effects of ambient versus physiological temperature on recycling kinetics.

Although many general-purpose simulation and analysis packages exist, most do not allow any alteration to the system during the course of an experimental assay. These alterations can include the addition and removal of reagents to extracellular media, and electrical stimulation of neurons being observed. None give a treatment of fluorescence which reflects our current understanding.

Debate is ongoing [2, 3] over which types of endocytosis may be in effect at CNS nerve terminals under different stimuli. A number of published computational models investigate the ability of one or a combination of these models to fit observed experimental data [15, 14]. However, these models are created on an ad-hoc basis for particular experimental protocols.

Additionally, different fluorescent markers have different properties and behaviours within these experimental assays. Generally, assays using one or other of these markers are modelled independently.

### 4 FM-Sim

We have developed FM-Sim with the intention of creating an easy-to-use application for the definition and simulation of fluorescence microscopy experiments. It is composed of a protocol definition user interface, a stochastic simulation engine, and a Bayesian inference engine to infer rate parameters for a protocol based on comparison with supplied observed data.

The simulation and inference engines use a model of vesicle movement within a nerve terminal, and can process the changes in rate which occur with changes in stimulus during a protocol, termed regime changes for the remainder of this paper. These regime changes are derived from the protocol definition, managing the effects of nested and overlapping events.

The flexibility of the protocol definition allows the wide variety of potential experiments to be modelled. New experiments can be simulated based upon rate parameters obtained from prior similar experiments.

### 4.1 FM-Sim Synaptic Terminal Model

At the core of FM-Sim is a stochastic model of vesicle movement, or more specifically the cell membrane making up the surface of vesicles, within a synaptic terminal. The model tracks the movement of cell membrane around the structures of a single synaptic terminal, namely the vesicles, endosomes and the plasma membrane. As a simplification, all membrane movements are tracked in quanta of vesicles as this is a consistent, smallest unit of membrane surface area to move. The plasma membrane is a repository of  $x$  vesicles worth of membrane, and endosomes are created with  $y$  vesicles worth of membrane and decrease in size as vesicles bud from their surface. Vesicles stored within the synaptic nerve terminal are designated as being part of the reserve pool (RP) or readily releasable pool (RRP).

The initiation of movement of vesicles between the regions (RP, RRP, endosomes, plasma membrane) is stochastic, with propensity defined by rules for each transition, as depicted in Figure 2.

However, in contrast to the widely-used convention in the simulation of stochastic chemical kinetics where the reaction events are abstracted as instantaneous, each of the processes moving vesicles from one state to another takes a non-negligible time. Therefore the model is extended to include delays. Each pool or region of vesicles has an associated transition state. Vesicles in this transition state take a fixed time to transition from their prior to their current state. This approach is a form of the Delayed Stochastic Simulation Algorithm (DSSA) as discussed in [4], with reactants being vesicles in the source region, and products being the vesicles transferred to the target region.

Let  $\mathcal{S}$  be the set of states in which a vesicle can exist

$$\mathcal{S} = \{RP, RRP, E, PM, Pre-RP, Pre-RRP, Pre-E, Pre-PM\}$$

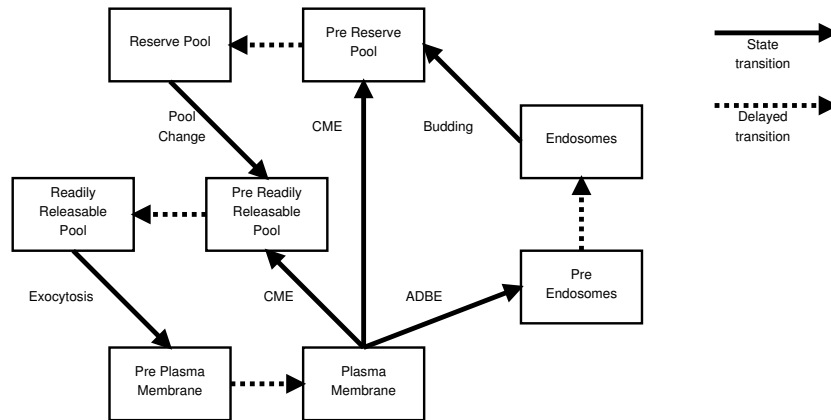


Fig. 2: FM-Sim synaptic terminal model.

denoting Reserve Pool, Readily Releasable Pool, Endosome, Plasma Membrane, and the associated pre-states respectively.

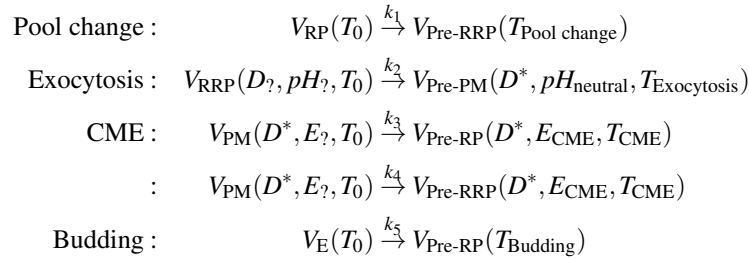
Define a vesicle as  $V_s(D, E, pH, T)$ ,  $s \in \mathcal{S}$  with the following properties:

- $D$  - Presence of FM dye: This determines whether or not the vesicle counts towards the fluorescence level of the nerve terminal. It is treated as a boolean value, as is the convention in current biological experiments. The dye is either present at the concentrations used when first loaded into the terminal ( $D_Y$ ), or completely absent ( $D_N$ ). Partial or low concentration dye loading does not take place.
- $E$  - Endocytosis source: The vesicle is classified as having been produced via recycling by CME ( $E_{CME}$ ) or ADBE ( $E_{ADBE}$ ). While it is possible that new vesicles could arrive from the soma of the cell, or be trafficked from neighbouring nerve terminals [10], it is thought that the effect of this possible influx of new vesicles occurs too slowly over the timeframe of an experiment to be detectable. The mechanism of vesicle creation is a factor in determining which vesicles fluoresce under the effect of each FM dye. FM2-10 has been shown to be taken up through CME only, whereas FM1-43 is taken up through both CME and ADBE at the loading concentrations commonly used in the literature. This differential take-up of different dyes was explored experimentally in depth in [7].
- $pH$ : Extracellular media is normally of neutral pH ( $pH_{neutral}$ , normalised to 1). Vesicles competent for release are at lower pH ( $pH_{acid}$ , normalised to 0). The reacidification process occurs between endocytosis and arrival at the vesicle pool. Experiments using pHluorins are affected by this pH change. Any pHluorins in contact with neutral pH fluoresce strongly, and this fluorescence decreases as the media within the vesicle is acidified. As experimental work has provided evidence that this reacidification process can take between three and five seconds [15, 3], pH levels are recorded as continuous values. After endocytosis, these values are reduced linearly over time to reach the target pH.
- $T$  - Time delay for vesicle to remain in pre-pool state as described above, with  $T_0$  representing 0 time delay.

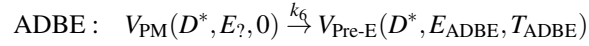
Note: for notational convenience, vesicle properties irrelevant to particular transitions may be omitted, for example  $V_s(D_Y) = V_s(D_Y, E?, pH?, T?)$ .

## 4.2 Discrete State Changes

The state changes of the model are:



$D^*$  represents that the vesicle is FM dye tagged *iff* FM dye is present in the extracellular media. There are two CME state changes, one for each destination pool, and each with a different propensity. Each of the rules above apply to individual vesicles for each instance of the rule being executed. The rule below however, operates on  $N$  vesicles taken together to represent a single endosome. If  $N$  vesicles are not available in the plasma membrane state, the rule will not be executed.



The values  $k_1, \dots, k_6$  are the rule propensities, each the product of the number of vesicles available in the source state, and a rule rate  $C$ . Let  $V$  denote number of vesicles:

$$\begin{aligned} k_1 &= V_{\text{RP}} \times C_{\text{Pool change}} \\ k_2 &= V_{\text{RRP}} \times C_{\text{Exocytosis}} \\ k_3 &= V_{\text{PM}} \times C_{\text{CME}} \times C_{\text{CME RP ratio}} \\ k_4 &= V_{\text{PM}} \times C_{\text{CME}} \times (1 - C_{\text{CME RP ratio}}) \\ k_5 &= V_{\text{E}} \times C_{\text{Budding}} \\ k_6 &= V_{\text{PM}} \times C_{\text{ADBE}} \end{aligned}$$

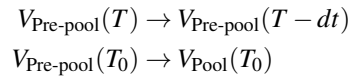
The values  $k_3$  and  $k_4$  have an additional input,  $C_{\text{CME RP ratio}}$ . This constant takes values from zero to one and represents the proportion of vesicles produced by CME which go to the RP. The remainder go to the RRP. In this work we will use 0.7 as the value for the  $C_{\text{CME RP ratio}}$ . Similar values are used in the literature [5].

In summary, the input parameters for the model are the rate constants  $C?$  and the time constants  $T?$ .

### 4.3 Continuous State Changes

In addition to the above state change rules, there are the following continuous processes:

- Pre-pool delays: A vesicle  $T_{\text{delay}} > 0$  reduces as simulated time elapses. Once the  $T_{\text{delay}}$  reaches  $T_0$ , a vesicle in a pre-pool moves into the corresponding pool



- Reacidification: The pH of a fully internalised vesicle or endosome (i.e. one which is no longer in direct contact with extracellular media) reduces linearly over time from  $pH_{\text{neutral}}$  to  $pH_{\text{acid}}$ , at a rate matching current literature [15, 3].



### 4.4 Fluorescence Calculation

The model can simulate the fluorescence of each of the three previously described fluorescent reporters. Based on the fluorescent reporter used in the experiment design, fluorescence is calculated as described below. In all cases fluorescence is scaled from minimum = 0 to maximum = 1 possible fluorescence by dividing by the total vesicle count in the model  $[V]$ .

- **FM1-43**: Total fluorescence is the count of all vesicles in states not in contact with extracellular media with FM dye boolean variable true. Vesicles in states {PM, Pre-PM} do not contribute because standard experimental protocols [20] have shown FM dye rapidly dissociates from the plasma membrane and is washed away in the extracellular media.

$$F_{\text{FM1-43}} = [V_s(D_Y)]/[V], s \notin \{\text{PM, Pre-PM}\}$$

- **FM2-10**: Total fluorescence is the count of all vesicles in the RP and RRP (and their pre-states) with vesicle source CME. ADBE-derived vesicles do not contribute under standard experimental protocols of 100 $\mu$ M FM2-10 [8].

$$F_{\text{FM2-10}} = [V_s(D_Y, E_{\text{CME}})]/[V], s \in \{\text{RP, RRP, Pre-RP, Pre-RRP}\}$$

- **pHluorin**: Total fluorescence is the sum of normalised vesicle pH of all vesicles. A family of pHluorin fusion proteins is commonly used in these experiments. For the purposes of simulation however, they are broadly the same in behaviour. They fluoresce when in contact with neutral pH and not when in an acidic environment. In addition to the normal physiological changes in pH within a nerve terminal, there are two external stimuli used in pHluorin assays.
  - *Ammonium addition*: Ammonium chloride is used to cause all pHluorin in a nerve terminal to fluoresce. When applied, ammonium ions permeate extracellular media, cytoplasm, and vesicle interiors, reducing the acidity of all media [19].
  - *Acid addition*: Impermanent acid is used to quench the fluorescence of pHluorin on the plasma membrane, leaving only the pHluorin on fully internalised membrane to fluoresce [3].

$$F_{\text{pHluorin}} = \begin{cases} 1, & \text{if } \text{NH}_4^+ \text{ present} \\ (\sum pH) / [V], & V_s(pH), s \notin \{\text{PM, Pre-PM}\} \text{ if acid present} \\ (\sum pH) / [V], & V_s(pH), s \in \mathcal{S} \text{ otherwise} \end{cases}$$

Current experimental data available records fluorescence levels per nerve terminal as relative measures only. It is not commonly feasible to calculate absolute quantities of marker. Therefore, experimental observations are taken to vary from maximum (1) and minimum (0) fluorescence per nerve terminal during the experimental assay.

#### 4.5 Protocol Definition and Rate Parameter Specification

FM-Sim allows the user to define an experimental protocol to a sufficient level of detail to be simulated. A protocol consists of a number of events with a defined start time (or frame) and a given duration. Multiple events may be active simultaneously, for example chemical stimulation of nerve terminals while simultaneously inhibiting certain protein functions within the nerve terminal with the application of chemical inhibitors. Figure 3 shows a defined example protocol.

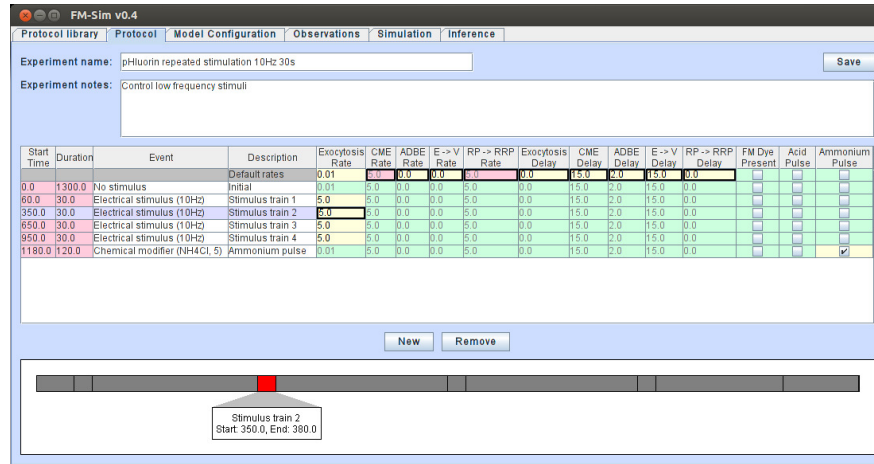


Fig. 3: A sample defined protocol in the FM-Sim protocol editor.

For each protocol event, the user may choose to enter values for rate parameters. The rate parameters available for modification depend on the configuration of the model to be simulated (discussed below). The user may also leave rate values for individual events unmodified, in which case the values are taken from the enclosing event if any, or a default rate if there are no enclosing events. Finally, the user may choose to mark rate parameters as to be inferred from observed data. This will require the loading of an appropriate dataset of observed fluorescence values for inference to be performed.

#### 4.6 Simulation

Given a defined experimental protocol, FM-Sim calculates the time-points at which regime changes occur. These are points when the kinetic rates of the model are allowed to change, at the start or end of protocol events. For example, the onset of low intensity electrical stimulation is expected to trigger exocytosis of synaptic vesicles, and compensatory clathrin mediated endocytosis.

These regime change time-points and the associated user-defined rates in effect during each regime are used to stochastically simulate a population of nerve terminals. The result is a trace of mean simulated fluorescence during the experiment.

The simulation engine uses an extended form of the Gillespie Stochastic Simulation Algorithm, specifically, the Direct Method [12], keeping track of vesicles and endosomes within a presynaptic terminal. The extensions added allow vesicle movement to be non-instantaneous using an algorithm similar to the DSSA method of [4], and handling of continuous state changes (pH) over time.

#### 4.7 Observation Data Handling

Observed experimental data may be input in the form of a comma-separated value (CSV) data file holding fluorescence values across multiple nerve terminal regions-of-interest (ROIs) over multiple imaging frames (usually one frame every few seconds).

Experimental fluorescence levels are known to decay during the time course of the experiment. This is due to photobleaching of the dye during image acquisition under the microscope. It is standard practice to compensate for this decay during analysis of experimental data, most commonly with a linear decay function. FM-Sim can apply a similar compensation formula to raw observed data if necessary:

$$\text{Corrected observation} = \text{Observation} - C \times (t_{\text{obs}} - t_0)$$

Where  $C$  is the linear correction factor,  $t_{\text{obs}}$  is the time of observation, and  $t_0$  is the time at the start of image acquisition. Generally, the linear correction factor is obtained by the user using calibration assays. If more complex decay correction is required, it is expected that the user performs the preprocessing prior to importing the data into FM-Sim. Once the data has been decay-corrected and scaled, it can be compared with the output of the simulation, or used to infer rate parameters.

#### 4.8 Bayesian Parameter Inference

We take a Bayesian approach to parameter inference, using a standard Particle Marginal Metropolis-Hastings (PMMH) scheme and Sequential Monte Carlo (SMC) estimates of marginal likelihoods [13, 1], with the addition of the following mechanism to handle regime changes. A defined protocol is decomposed into rate change events. The minimum set of inference parameters is also calculated over the entire protocol. For each PMMH iteration, a set of proposals are drawn for the set of inference parameters. The SMC scheme is then run, changing the rates in effect as each rate change time is reached in the simulation.

The SMC scheme used in FM-Sim is as described by Golightly *et al.* [13]. It requires a set of  $N$  particles generated by forward simulation for each observed time-point. The weight  $w$  of each of these particles contributes to the estimated marginal likelihood  $\hat{p}(y_{t+1}|\mathbf{y}_t, c)$  where  $y_{t+1}$  is the experimental observation at time  $t + 1$ ,  $\mathbf{y}_t$  is the set of experimental observations up to time  $t$ , and  $c$  is the set of simulation parameters.

$$\hat{p}(y_{t+1}|\mathbf{y}_t, c) = \frac{1}{N} \sum_{i=1}^N w_{t+1}^i \quad \text{where} \quad w_t^i = p(y_t|x_t^i, c)$$

The overall estimated marginal likelihood of the SMC scheme is the product of the marginal likelihoods of all of the  $T$  observed time-points

$$\begin{aligned} \hat{p}(\mathbf{y}|c) &= \hat{p}(y_1|c) \prod_{t=1}^{T-1} \hat{p}(y_{t+1}|\mathbf{y}_t, c) \\ &= \prod_{t=1}^T \frac{1}{N} \sum_{i=1}^N p(y_t|x_t^i, c) \end{aligned}$$

Each particle weight is  $p(y_t|x_t^i, c)$ , where  $y_t$  is the experimentally observed (normalised) fluorescence at time  $t$ ,  $x_t^i$  is the fluorescence of simulated particle  $i$  at time  $t$ , and  $c$  is the set of simulation parameters. In other words, the probability of obtaining values matching the observed  $y_t$  given the simulated result  $x_t$ , making the assumption that  $p(y_t|x_t^i, c) = p(y_t|x_t^i)$ .

The calculations also make the assumption that both the experimental and simulated observations at a particular time-point are normally distributed. Experimental observations provide a set of fluorescence values for  $y_t$ , from which we can compute a mean  $\mu(y_t)$  and variance  $\sigma(y_t)^2$ . Forward simulation of an individual particle provides a single value for  $x_t^i$ . Given that the single particle result has zero variance,  $\mathcal{N}(\mu(y_t)|x_t^i, \sigma(x_t^i)^2)$  is not useful.

To avoid this problem, we make the assumption that the variance around an  $x_t^i$  result is equal to the variance of the observed  $y_t$  values. This has the advantage over choosing an arbitrary variance that it provides a variance for each time-point which is tailored to the experimental data. This provides the distribution

$$\mathcal{N}(\mu(y_t)|x_t^i, \sigma(y_t)^2) = \mathcal{N}(x_t^i|\mu(y_t), \sigma(y_t)^2)$$

Finally, the distribution is normalised to the peak probability  $\mathcal{N}(\mu(y_t)|\mu(y_t), \sigma(y_t)^2)$  to avoid arithmetic underflow of marginal likelihoods of long time-series, and to provide a more user-friendly distance measure. As PMMH proposal acceptance probability is based on the ratio of proposal marginal likelihood over the previously accepted marginal likelihood, this normalisation of the whole time series has no effect on proposal acceptance.

$$\begin{aligned} p(y_t|x_t^i, c) &= \frac{\mathcal{N}(x_t^i|\mu(y_t), \sigma(y_t)^2)}{\mathcal{N}(\mu(y_t)|\mu(y_t), \sigma(y_t)^2)} \\ &= \exp\left(-\frac{x_t^i - \mu(y_t)}{2\sigma(y_t)^2}\right) \end{aligned}$$

The marginal likelihood of each run of the SMC scheme is used to update the PMMH best match for that iteration.

The final result of the inference process is a set of rate parameters across the whole protocol which was the best match for the experimental data which was found for the model in use. For most applications, it is expected that there will be a mix of user-defined and inferred rate parameter values.

## 5 Case Study 1: FM Dye based assay

This case study uses real experimental data from the Cousin neuronal cell biology laboratory in Edinburgh [5]. The assay has multiple exocytosis stimuli designed to trigger release of synaptic vesicles from both of the vesicle pools (RP and RRP). The case study demonstrates use of FM dyes, regime changes and a series of protocol events, shown in Table 1. The raw observations are corrected for decay with a linear correction of 200 fluorescence units per second.

Table 1: Protocol events for the FM dye based assay.

| Event      | Stimulus               | Start time (s) | Duration (s) |
|------------|------------------------|----------------|--------------|
| Default    | None                   | 0              | 250          |
| RRP Unload | Electrical (20Hz)      | 12             | 2            |
| RP Unload  | Chemical (KCl, 0.5 mM) | 100            | 30           |

This first example shows inferred parameters for a model without ADBE. The inference parameters were Exocytosis, CME, and Pool Change rate, for each of the three protocol events. The remaining parameters were fixed. The final results of inference are shown in Figure 4a, leading to the parameters shown in Table 2, with a distance measure of -0.35.

Repeating the inference with allowing the parameters ADBE and Budding rate to be inferred under the second stimulus gave the parameters shown also in Table 2, with an improved distance measure of -0.22, illustrated in Figure 4b.

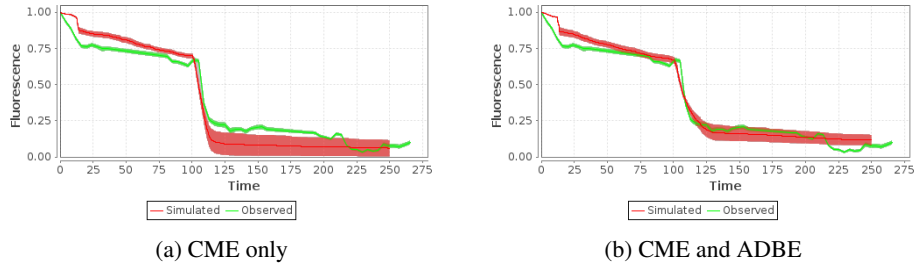


Fig. 4: Simulated fluorescence traces using the inferred parameters shown in Table 2, plotted against the real observed data used for parameter inference.

Table 2: Inference results for CME only, and both CME and ADBE. Values shown are rate constants  $C$  ( $s^{-1}$ ) and time delay constants  $T$  (s) for each of the discrete state change rules, with inferred values shown in bold.

| Event               | Exocytosis   |     | CME         |     | ADBE        |     | Budding     |     | Pool change |     |
|---------------------|--------------|-----|-------------|-----|-------------|-----|-------------|-----|-------------|-----|
|                     | $C$          | $T$ | $C$         | $T$ | $C$         | $T$ | $C$         | $T$ | $C$         | $T$ |
| <b>CME only</b>     |              |     |             |     |             |     |             |     |             |     |
| Default             | <b>0.03</b>  | 0   | <b>0.01</b> | 15  | 0           | 2   | 0           | 15  | <b>0.00</b> | 1   |
| RRP Unload          | <b>8.81</b>  | 0   | <b>1.67</b> | 15  | 0           | 2   | 0           | 15  | <b>0.92</b> | 1   |
| RP Unload           | <b>8.23</b>  | 0   | <b>0.84</b> | 15  | 0           | 2   | 0           | 15  | <b>1.00</b> | 1   |
| <b>CME and ADBE</b> |              |     |             |     |             |     |             |     |             |     |
| Default             | <b>0.04</b>  | 0   | <b>0.01</b> | 15  | 0           | 2   | <b>0.07</b> | 15  | <b>0.00</b> | 1   |
| RRP Unload          | <b>10.29</b> | 0   | <b>0.87</b> | 15  | 0           | 2   | <b>0.01</b> | 15  | <b>3.50</b> | 1   |
| RP Unload           | <b>4.03</b>  | 0   | <b>1.06</b> | 15  | <b>0.58</b> | 2   | <b>0.87</b> | 15  | <b>0.36</b> | 1   |

## 6 Case Study 2: pHluorin Based Assay

This case study is based on current pHluorin experimental work from the Cousin laboratory. The assay demonstrates repeated stimulus and recovery cycles, along with the use of pHluorin specific stimulus, shown in Table 3. Again, real experimental observations have been used.

Final results of inference as shown in Figure 5, gave the parameters shown in Table 4, with a distance measure of -7.14.

## 7 Conclusions

The FM-Sim application and its computational model of synaptic vesicle recycling has been demonstrated to work for a number of experimental assays. It provides the following benefits to both experimental and theoretical neuroscientists

- A user-friendly means of cataloguing experimental assays.
- An aid to experimental design by simulating the predicted effects of chemical modifiers on neurons prior to *in vitro* work.
- A means of gaining further insight into the kinetics of vesicle recycling by having numerous sets of observed data compared against a single kinetic model. This allows validation of the model and its rate parameters under a range of environmental conditions.

Table 3: Protocol events for the pHluorin Based Assay.

| Event            | Stimulus                             | Start time (s) | Duration (s) |
|------------------|--------------------------------------|----------------|--------------|
| Rest             | None                                 | 0              | 1300         |
| Stimulus train 1 | Electrical (10Hz)                    | 60             | 30           |
| Stimulus train 2 | Electrical (10Hz)                    | 350            | 30           |
| Stimulus train 3 | Electrical (10Hz)                    | 650            | 30           |
| Stimulus train 4 | Electrical (10Hz)                    | 950            | 30           |
| Ammonium pulse   | Chemical (NH <sub>4</sub> Cl, 50 mM) | 1180           | 120          |

Table 4: Inference Results for pHluorin Assay. Values shown are rate constants  $C$  (s<sup>-1</sup>) and time delay constants  $T$  (s) for each of the discrete state change rules, with inferred values shown in bold.

| Event            | Exocytosis  |     | CME         |     | ADBE |     | Budding |     | Pool change  |     |
|------------------|-------------|-----|-------------|-----|------|-----|---------|-----|--------------|-----|
|                  | $C$         | $T$ | $C$         | $T$ | $C$  | $T$ | $C$     | $T$ | $C$          | $T$ |
| Rest             | 0.01        | 0   | <b>2.59</b> | 15  | 0    | 2   | 0       | 15  | <b>10.34</b> | 0   |
| Stimulus train 1 | <b>4.81</b> | 0   | <b>2.59</b> | 15  | 0    | 2   | 0       | 15  | <b>10.34</b> | 0   |
| Stimulus train 2 | <b>8.12</b> | 0   | <b>2.59</b> | 15  | 0    | 2   | 0       | 15  | <b>10.34</b> | 0   |
| Stimulus train 3 | <b>3.68</b> | 0   | <b>2.59</b> | 15  | 0    | 2   | 0       | 15  | <b>10.34</b> | 0   |
| Stimulus train 4 | <b>5.59</b> | 0   | <b>2.59</b> | 15  | 0    | 2   | 0       | 15  | <b>10.34</b> | 0   |
| Ammonium pulse   | 0.01        | 0   | <b>2.59</b> | 15  | 0    | 2   | 0       | 15  | <b>10.34</b> | 0   |

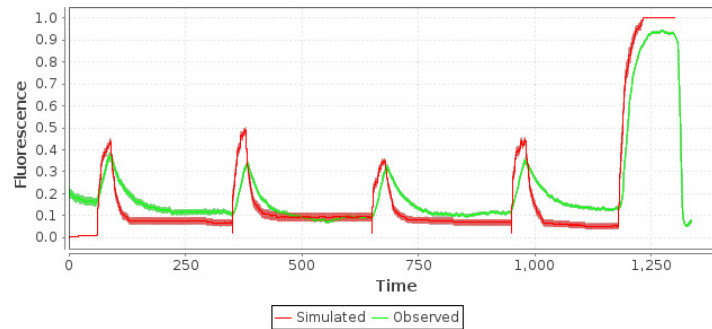


Fig. 5: Simulated fluorescence trace using the inferred parameters shown in Table 4, plotted against the real observed data used for parameter inference.

FM-Sim is currently being applied to a range of experimental assays within the Cousin laboratory at the University of Edinburgh. The research focus of this laboratory includes investigation of the mechanisms involved in synaptic vesicle recycling. Future work includes extending this library of experimental protocols, with supporting experimental data. In addition, we intend to cross-validate inferred experimental rates and models between compatible experiments, where environmental factors allow.

Further refinement of the model is also intended. In particular, ADBE derived vesicles are theorised to be processed by a number of sorting endosomes, modifying the complement of membrane proteins in the processed vesicle [6]. The computational model attempts to replicate these mechanisms to determine if such refinements improve the fit to observed data.

FM-Sim is available at <http://homepages.inf.ed.ac.uk/s9269200/software/>.

**Acknowledgements** Thanks to the members of the Cousin group, in particular Sarah Gordon, for helpful discussions, and provision of experimental data. Thanks also to the reviewers of this paper for their helpful comments and suggestions.

This work was supported in part by grants EP/F500385/1 and BB/F529254/1 for the University of Edinburgh School of Informatics Doctoral Training Centre in Neuroinformatics and Computational Neuroscience ([www.anc.ac.uk/dtc](http://www.anc.ac.uk/dtc)) from the UK Engineering and Physical Sciences Research Council (EPSRC), UK Biotechnology and Biological Sciences Research Council (BBSRC), and the UK Medical Research Council (MRC). The work has made use of resources provided by the Edinburgh Compute and Data Facility (ECDF; [www.ecdf.ed.ac.uk](http://www.ecdf.ed.ac.uk)), which has support from the eDIKT initiative ([www.edikt.org.uk](http://www.edikt.org.uk)).

Stephen Gilmore is supported by the BBSRC SysMIC grant, BB/I014713/1.

## References

1. Andrieu, C., Doucet, A., Holenstein, R.: Particle Markov chain Monte Carlo methods. *Journal of the Royal Statistical Society: Series B (Statistical Methodology)* 72(3), 269–342

- (2010)
2. Aravanis, A., Pyle, J., Tsien, R.: Single synaptic vesicles fusing transiently and successively without loss of identity. *Nature* 423(6940), 643–647 (2003)
  3. Atluri, P.P., Ryan, T.A.: The kinetics of synaptic vesicle reacidification at hippocampal nerve terminals. *The Journal of Neuroscience* 26(8), 2313–2320 (2006)
  4. Barrio, M., Burrage, K., Leier, A., Tian, T.: Oscillatory regulation of Hes1: discrete stochastic delay modelling and simulation. *PLoS Computational Biology* 2(9), e117 (2006)
  5. Cheung, G., Jupp, O., Cousin, M.: Activity-Dependent bulk endocytosis and clathrin-dependent endocytosis replenish specific synaptic vesicle pools in central nerve terminals. *The Journal of Neuroscience* 30(24), 8151–8161 (2010)
  6. Cheung, G., Cousin, M.A.: Adaptor Protein Complexes 1 and 3 Are Essential for Generation of Synaptic Vesicles from Activity-Dependent Bulk Endosomes. *The Journal of Neuroscience* 32(17), 6014–6023 (2012)
  7. Clayton, E., Cousin, M.: Differential labelling of bulk endocytosis in nerve terminals by FM dyes. *Neurochemistry International* 53(3), 51–55 (2008)
  8. Cousin, M.: Use of FM1-43 and Other Derivatives to Investigate Neuronal Function. *Current Protocols in Neuroscience* pp. 2–6 (2008)
  9. Cousin, M.: Activity-dependent bulk synaptic vesicle endocytosis - a fast, high capacity membrane retrieval mechanism. *Molecular Neurobiology* 39(3), 185–189 (2009)
  10. Fernandez-Alfonso, T., Ryan, T.A.: A heterogeneous “resting” pool of synaptic vesicles that is dynamically interchanged across boutons in mammalian CNS synapses. *Brain Cell Biology* 36(1), 87–100 (2008)
  11. Gabriel, T., García-Pérez, E., Mahfooz, K., Goñi, J., Martínez-Turrillas, R., Pérez-Otaño, I., Lo, D., Wesseling, J.: A new kinetic framework for synaptic vesicle trafficking tested in synapsin knock-outs. *The Journal of Neuroscience* 31(32), 11563–11577 (2011)
  12. Gillespie, D.: Exact stochastic simulation of coupled chemical reactions. *The Journal of Physical Chemistry* 81(25), 2340–2361 (1977)
  13. Golightly, A., Wilkinson, D.: Bayesian parameter inference for stochastic biochemical network models using particle Markov chain Monte Carlo. *Interface Focus* 1(6), 807–820 (2011)
  14. Granseth, B., Lagnado, L.: The role of endocytosis in regulating the strength of hippocampal synapses. *The Journal of Physiology* 586(24), 5969–5982 (2008)
  15. Granseth, B., Odermatt, B., Royle, S.J., Lagnado, L.: Clathrin-mediated endocytosis is the dominant mechanism of vesicle retrieval at hippocampal synapses. *Neuron* 51(6), 773–786 (2006)
  16. McMahon, H., Boucrot, E.: Molecular mechanism and physiological functions of clathrin-mediated endocytosis. *Nature Reviews Molecular Cell Biology* 12(8), 517–533 (2011)
  17. Miesenböck, G., De Angelis, D.A., Rothman, J.E.: Visualizing secretion and synaptic transmission with pH-sensitive green fluorescent proteins. *Nature* 394(6689), 192–195 (1998)
  18. Royle, S., Granseth, B., Odermatt, B., Derevier, A., Lagnado, L.: Imaging pHluorin-based probes at hippocampal synapses. *Methods in Molecular Biology* 457, 293–303 (2008)
  19. Sankaranarayanan, S., De Angelis, D., Rothman, J., Ryan, T.: The use of pHluorins for optical measurements of presynaptic activity. *Biophysical Journal* 79(4), 2199–2208 (2000)
  20. Wu, Y., Yeh, F., Mao, F., Chapman, E.: Biophysical characterization of styryl dye-membrane interactions. *Biophysical Journal* 97(1), 101–109 (2009)